Machine Learning Based Cell Model for fast approximation of cellular action potential to enable clinical translation

Pau Romero, Miguel Lozano, Giada Romitti, Dolors Serra, Ignacio Garcia-Fernandez, Alejandro Liberos, Miguel Rodrigo, Rafael Sebastian

CoMMLab, Universitat de Valencia, Valencia, Valencia, Spain

Abstract

Simulations of cardiac arrhythmias have shown great potential to plan and optimize therapies. However, biophysical models are complex and involve a high computational cost that poses a problem for their clinical translations. Alternative methods such as Eikonal based simulations can help to reduce the cost at the expense of not considering an action potential model. In this work, we present a methodology to predict the action potential curves during Eikonal simulations. We first train a model with data obtained from biophysical simulations, and following we test their ability to obtain realistic action potentials, given a cell state and the diastolic intervals. A simulation study shown that this method is able to reproduce action potentials in a tissue slab during rotor activity and different stimulation protocols, avoiding to solve ionic models, and reducing dramatically the computational cost.

1. Introduction

Multi-scale models for heart electrophysiology have shown a great potential to study complex mechanisms and interactions occurring in cardiac tissue [1]. At organ level, the use of heart models that include the properties of heterogeneous tissue and pathological substrates have been proposed to study the vulnerability to arrhythmias and optimize therapies such as catheter based ablation [2]. It is common to base those simulations on the monodomain model (tissue level) coupled to detailed cell (ionic) models that include a high level of detail at subcellular level, and require to solve a large number of ordinary differential equations with short time steps (order of microseconds). When those models have to be solved on a full heart finite element model, they impose additional constraints on mesh resolution, that imply large computational cost that make them impractical for clinical environments.

Several solutions have been presented, which include the use of GPU-based solvers that can reduce the computational time [3], the use of minimal ionic models [4, 5], or the use of phenomenological models [6]. To simulate electrical diffusion on cardiac tissue, Eikonal models and cellular automaton have been proposed to reduce the computational cost, when subcellular interactions can be neglected [7]. However, most implementations do not take into account the detailed dynamic response of cells, that can change action potential (AP) morphology and duration, as a function of diastolic interval (DI) and previous cell state (AP memory).

In this study, we propose the use of the Eikonal model at tissue level coupled to a cellular automaton that has been trained with APs obtained from biophysical simulations for a variety of cell types, and can produce realistic APs (not only restitution curves) for changing conditions with very low computational cost. First, we perform a simulation study to generate APs that result from S1 and S1-S2 stimulation protocols. Following, we characterize the APs and learn the relationship between current cell state, DI and next cell AP. Finally, we assess the accuracy of the estimation in tissue simulations, including rotor activity.

2. Material and Methods

In order to produce complete APs without the need of solving any equation at cell level, we have formulated the problem as a set of dynamic cell states that give rise to the AP curves. Therefore, a simulation of a given cell AP can be seen as a succession of states $\{s_i\}_{i=0}^{n}$. According to this approach, given an initial cell state, s_0, and a series of activation times, $\{t_i\}_{i=0}^{n}$, the simulation of a cell AP can be modeled as the problem of predicting the successive states $\{s_i\}_{i=1}^{n}$.

We define the function $next(s_t, di_t) = s_{t+1}$, which depends on the current cell state, and the DI to obtain the next state that will define the corresponding AP. We assume that a cell in a state x_t will be activated at time t_{act}, so that we can obtain di_t (di_t = t_{act} - $apd90_{time}(x_t)$).

We built a dataset from biophysical simulations with the aim to create a large dataset of AP curves, together with the corresponding DI values, and the resulting previous and next states, i.e. AP curves.

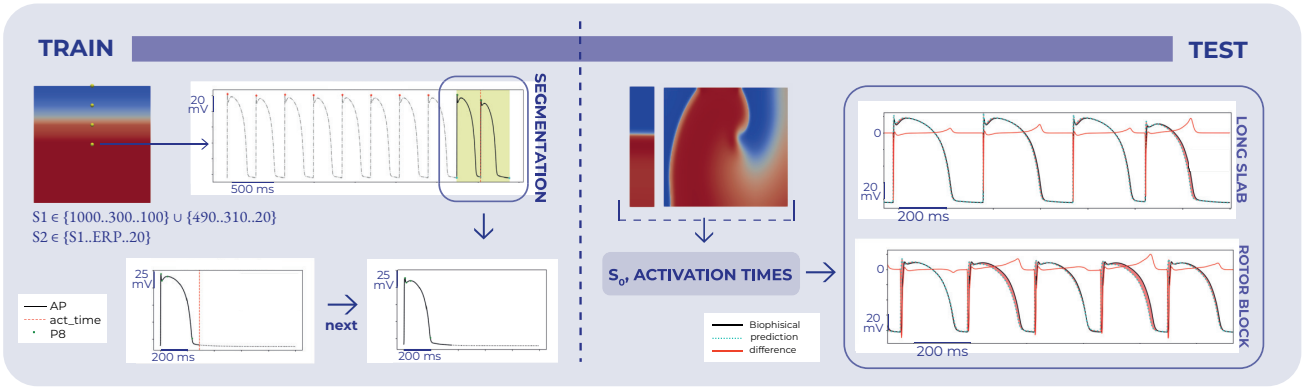

Figure 1. Graphic description of the proposed approach. It is divided in a training phase based on output of biophysical simulations and a test phase where the model is used to predict the corresponding AP for each cell in an Eikonal based simulation.

2.1. Generation of electrophysiological data

We performed a simulation study on three different 3D tissue blocks to obtain the AP curves dataset for training and testing. We considered six cell types: endocardium (ENDO), mid-myocardium (MID), and epicardium(EPI) in healthy conditions, and remodeled conditions due to infarction (border zone, BZ). We based our simulation study in the ten Tusscher ionic model [8] at cell level, and the monodomain model at tissue level. The simulations were performed with the cardiac biophysical solver ELVIRA [9], applying the conjugate gradient method with an integration time step (dt) of 0.02 ms to compute the numerical solution.

To build the training set, we used a block of dimensions $3 \times 3 \times 0.25$ mm for each cell type. Then, we stimulated each tissue block with BCLs ranging from 300 ms to 1000 ms with steps of 100 ms, and from 310ms to 490ms with steps of 20. This configuration allowed us to obtain the relationship between DI and AP with a constant BCL. Following, we carried out a S1-S2 protocol, in which we first stabilized the simulation to a constant BCL (S1), to then trigger an activation with a shorter CL (S2). S2 ranged from S1 value, to the minimum possible coupled stimulus that depended on the effective refractory period. During the simulation we recorded the AP at four locations (probes) aligned on the center of the the tissue block with a temporal resolution of $20\mu s$.

To generate the test data, we designed two scenarios changing both the stimulation protocol and the geometry to measure the capacity of generalization of the prediction model to different conditions. In both cases, the AP curves were recorded for all the points in the geometry with a time resolution of 1ms. For the first scenario we built a long slab of tissue of dimensions, $3 \times 20 \times 0.25$ mm. We applied an S1-S2 activation protocol with values different from the ones used in the test set. Namely, for ENDO and EPI S1$=$ 380, and S2$\in$ $\{360, 340, 320\}$, and for MID, ENDO BZ, MID BZ and EPI BZ, S1$=$ 380, and S2$\in$ $\{360, 340, 320\}$. For the second scenario, we used a squared EPI tissue block of dimensions $50 \times 50 \times 0.03$ mm where we generated a stabilized rotor and recorded the last 5000ms.

2.2. Segmentation and encoding of the action potential curves

To build the training set, two main steps were carried out: i) segmentation of the last two stimuli of each train of the S1-S2 protocol, and ii) encoding of the AP curve in a compact representation. Figure 1 contains a graphical description of this procedure.

The segmentation step, started with the detection of the minimum and maximum peaks of the AP curves. Then, only the stimulus corresponding to the last S1, and S2 were processed. To store them in the AP curve data set, we reformatted all the stimuli to 1000ms (sampled at 0.02 ms). Therefore, curves database was built with the 3-tuple $(t_i, AP_i, next(AP_i))$ elements.

Once the AP data set was built, each of the curves was encoded by a feature vector built with 4 characteristic points, $(t, AP(t))$, of the AP curves. The selected points were: i) the upstroke peak, ii) the local minimum following the spike, iii) the maximum of the plateau phase, and iv) the point at 90% of the repolarization (APD_{90}).

A cell state $s = (t_1, t_2, t_3, t_4, ap_1, ap_2, ap_3, ap_4)$, is 8 dimension vector with the coordinates of the 4 selected points (t_i, ap_i) captured from an AP curve. We then build another data set, retaining the index order of the previous one, made of the encoded AP curves. Therefore, the elements of the data set were as follow: $(t_i, s_i, next(t_i, s_i))$.

As we aimed to learn cell-state transitions from a pair,

DI, state, (di, s), from the last dataset, we built the matrix, X=(di_i, s_i) and Y=$(next(s_i))$, by computing the DI of each element and replacing t_i with di_i.

2.3. Action potential estimation

Although we consider a machine learning based regression model, we finally chose an approach based on finding the *nearest transition* from the dataset. Note that a sample $s \in X$ contains data from different nature and scales (di and 4 points $(t, ap(t))$), and distance based ML-models improperly weight the feature vectors producing inadequate results. In addition, the morphology differences between the states involved in a transition sample $s \rightarrow s_{t+1}$ are generally reduced, however the diastolic interval has a higher influence. Finally, big datasets of transition samples $(X \rightarrow Y)$ can be generated from a biophysical simulators so, to build a search-model able to find the nearest (di_i, s_i) from the dataset and then simply return the corresponding $next(di_i, s_i)$ seems a robust strategy compared to regression models that try to approximate $next(di_i, s_i)$.

When a new cell activation is produced, the activation time (act_t) is used to calculate the new and then, the cell can compute its $next$ state. We have split $next$ function in two sequential Nearest Neighbors (NN) search steps. Firstly, we perform a NN-search exclusively with the di_t received on X, and keep the first k-neighbors. Secondly, the current cell state, x_t, is now used to find its NN among the states selected in the previous step. Finally, the index (from the dataset) of the nearest di-state tuple found is used by the $next$ function to return the corresponding state in Y as the new cell state s_{t+1}.

3. Results

To assess the accuracy of the proposed model, we designed two scenarios of test. In both the geometry and the activation protocol differ from the ones used to build the training set, for more details of both refer to section 2.

In table 1, there can be found the mean and standard deviation of the absolute error of all the tissue types and for all the test simulations carried out on the long tissue slab. Although all errors have low mean absolute errors, the standard deviation presents high values for all the tissue types, specially for the ENDO in both healthy and BZ. This high standard deviation is explained by the big and local peaks of error than can be appreciated in the AP curves plots in Figure 1. The main source of error is due to the delay of around 1 ms that occurs during the fast depolarization, and during the end of the repolarization were the curve slope of the function makes a sharp bend. This phenomenon of local error due to curve misalignment can be appreciated in Figure 2 where some regions of the activation front show a small delay.

Cell Type	MAE	STD	Cell Type	MAE	STD
ENDO	1.59	13.46	ENDO BZ	3.41	8.21
MID	0.93	4.83	MID BZ	1.31	7.69
EPI	1.68	5.31	EPI BZ	1.89	4.97

Table 1. Mean and standard deviation of the absolute error (in mV) computed over each point of the test mesh during each of the test stimulus of the pacing protocol. MAE: Mean absolute error, STD: Standard deviation

The last test scenario consists of the simulation of a self sustained rotor. This scenario pushes the generalization of the model to the limit, since the AP curves changes its morphology under such extreme circumstances slowing the depolarization, as can be seen in figure 3. However the model showed a performance similar to the slab scenario, proving its robustness with a mean absolute error of 1.03 mV with an standard deviation of 15.76 mV. By visual inspection of Figure 3, it can be appreciated that the activation front presents the same error as the one it presented on the slab.

4. Conclusions

We have presented a methodology for approximation of the AP curves based on a model that has been trained with a large number of biophysical simulations. The model is able to approximate the AP curves in simplified simulations based on Eikonal diffusion, including complex scenarios such as rotors. This approach might facilitate the clinical translation of simulations for therapy planning of catheter based interventions.

Acknowledgments

This research was funded by Generalitat Valenciana Grant AICO/2021/318 (Consolidables 2021) and Grant PID2020-114291RB-I00 funded by MCIN/ 10.13039/ 501100011033 and by "ERDF A way of making Europe"; D.S. was funded by ACIF/2021/394, Valencian Community (Spain);

References

[1] Trayanova NA, Boyle PM. Advances in modeling ventricular arrhythmias: from mechanisms to the clinic. Wiley Interdiscip Rev Syst Biol Med 2014;6(2):209–24.

[2] Lopez-Perez A, Sebastian R, Izquierdo M, Ruiz R, Bishop M, Ferrero JM. Personalized cardiac computational models: From clinical data to simulation of infarct-related ventricular tachycardia. Frontiers in Physiology 2019;10:580. ISSN 1664-042X.

[3] Sachetto Oliveira R, Martins Rocha B, Burgarelli D, Meira Jr W, Constantinides C, Weber Dos Santos R. Performance evaluation of gpu parallelization, space-time adaptive algorithms, and their combination for simulating cardiac electrophysiology. Int J Numer Method Biomed Eng 02 2018;34(2).

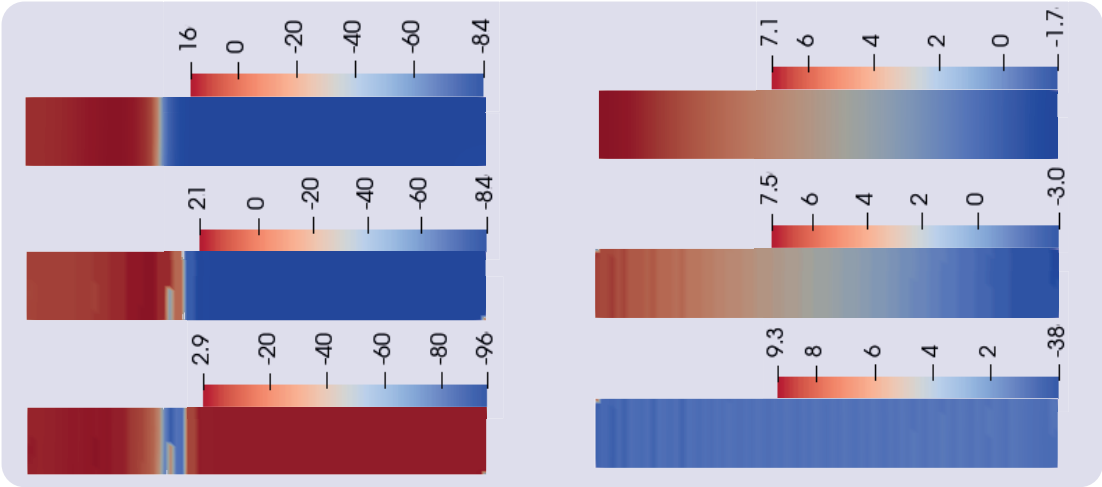

Figure 2. Comparison of the simulation on the slab of tissue at two different time instants. From top to bottom, simulations for biophysical model, the prediction model and their difference. All data is provided in mV.

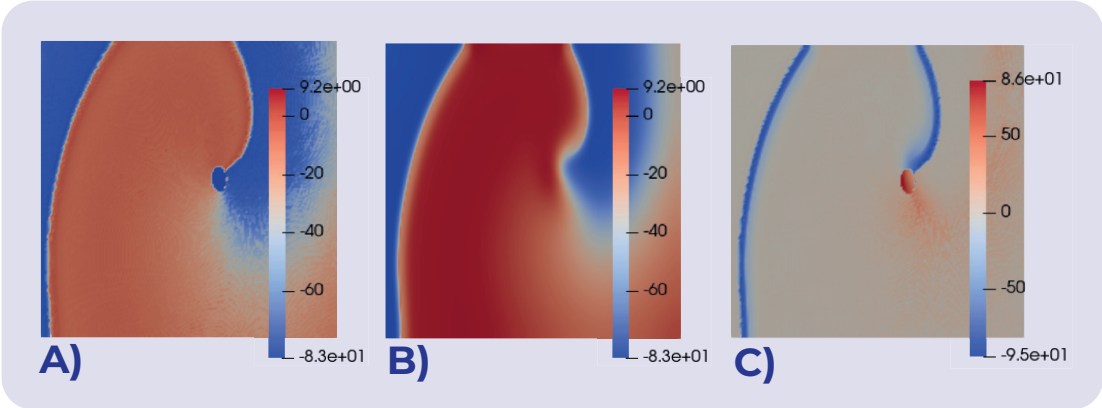

Figure 3. Comparison of the rotor simulation. In a) the prediction model, in b) the biophysical model, c) the difference. All data is provided in mV.

[4] Mitchell CC, Schaeffer DG. A two-current model for the dynamics of cardiac membrane. Bulletin of mathematical biology 2003;65(5):767–793.

[5] Bueno-Orovio A, Cherry EM, Fenton FH. Minimal model for human ventricular action potentials in tissue. J Theor Biol Aug 2008;253(3):544–60.

[6] Relan J, Chinchapatnam P, Sermesant M, Rhode K, Ginks M, Delingette H, Rinaldi CA, Razavi R, Ayache N. Coupled personalization of cardiac electrophysiology models for prediction of ischaemic ventricular tachycardia. Interface Focus Jun 2011;1(3):396–407.

[7] Serra D, Romero P, Garcia-Fernandez I, Lozano M, Liberos A, Rodrigo M, Bueno-Orovio A, Berruezo A, Sebastian R. An automata-based cardiac electrophysiology simulator to assess arrhythmia inducibility. Mathematics 2022;10(8). ISSN 2227-7390.

[8] Tusscher KHT, Panfilov AV. Cell model for efficient simulation of wave propagation in human ventricular tissue under normal and pathological conditions. Phys Med Biol December 2006;51(23):6141–6156.

[9] Heidenreich E, Ferrero JM, Doblare M, Rodriguez JF. Adaptive macro finite elements for the numerical solution of monodomain equation in cardiac electrophysiology. Annals of biomedical engineering 2010;38:2331–2345.